Supporting Information

Rational Design of a Redox-Active Nonaqueous Electrolyte for a High-Energy-Density Supercapacitor Based on Carbon Nanotubes

Jinwoo Park,[†] *Young-Eun Yoo,*[†] *Liqiang Mai,*[‡] *and Woong Kim*[*,†]

[†] Department of Materials Science and Engineering, Korea University, 145 Anam-ro, Seongbuk-gu, Seoul 02841, Republic of Korea

[‡] State Key Laboratory of Advanced Technologies for Materials Synthesis and Processing, International School of Materials Science and Engineering, Wuhan University of Technology, 122 Luoshi Road, Wuhan 430070, P.R. China

*E-mail: woongkim@korea.ac.kr (W. Kim)

Table of Contents

Total number of pages: 12

Total number of figures: 5

Total number of tables: 1

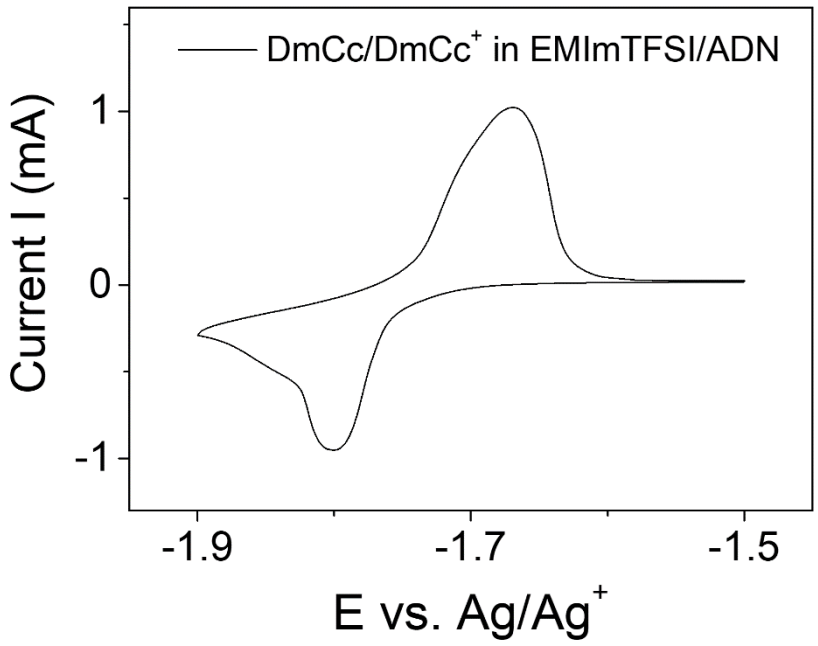

Figure S1. A CV conditioning process with a three-electrode configuration.

A conditioning process has been performed with a three-electrode configuration for stabilization of system. The entire process was conducted in the argon-filled glove box (water and oxygen < 1 ppm). The SWNT electrode was used as a working electrode. The high mass activated carbon (~10 mg cm^{-2}, 8:1:1 = YP-50F : Super-P : polyvinylidene fluoride) was used as a counter electrode material for the smooth voltage shift.[1] The CV was scanned in the range of -1.9 to -1.5 V *vs.* Ag/Ag^+ at a scan rate of 0.1 mV s^{-1}. After seven cycles, the working electrode was removed and used as the negative electrode of the two-electrode cell, where another SWNT electrode was used as the positive electrode.

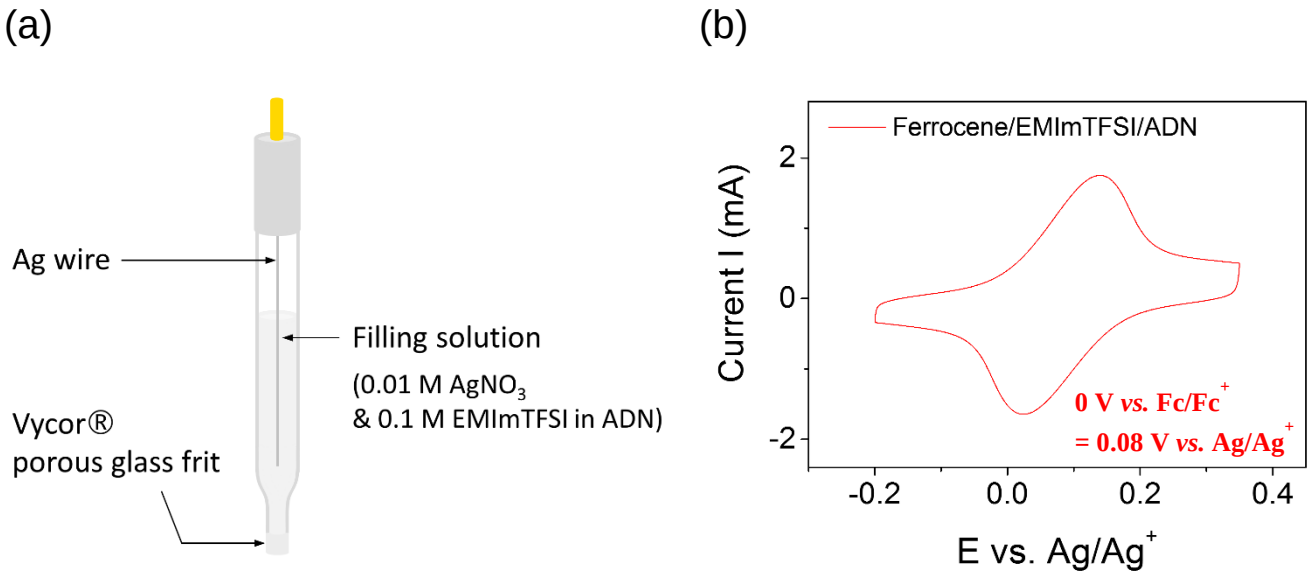

Figure S2. (a) Schematic of an Ag/Ag^+ reference electrode with filling solution for non-aqueous electrolytes. (b) A CV test with 10 mM ferrocene in 0.5 M EMImTFSI in ADN at v = 10 mV s^{-1} (working, counter, and reference electrodes are SWNT, activated carbon, and Ag/Ag^+ electrode, respectively).

Equations

The non-linear galvanostatic charge-discharge (GCD) characteristics of RAESs are calculated by the integration of GCD curves for the realistic evaluation.

Electrode capacitance (C_{elec+} or C_{elec-}, F)

$$C_{elec} = \frac{I}{dV/dt} = \frac{I\int V\,dt}{\int V\,dV} = \frac{I\int V\,dt}{V^2/2|_0^{\Delta V}} = \frac{2I\int V\,dt}{V^2|_0^{\Delta V}} \quad \cdots \quad \text{(Equation S1)}$$

Cell capacitance (C, F)

$$\frac{1}{C} = \frac{1}{C_{elec+}} + \frac{1}{C_{elec-}} \quad \cdots \quad \text{(Equation S2)}$$

Specific cell capacitance (C_{cell}, F g^{-1}) from GCD curves

$$C_{cell} = \frac{I}{2m \cdot dV/dt} = \frac{I\int V\,dt}{2m \cdot \int V\,dV} = \frac{I\int V\,dt}{2m \cdot V^2/2|_0^{\Delta V}} = \frac{2I\int V\,dt}{2m \cdot V^2|_0^{\Delta V}} \quad \cdots \quad \text{(Equation S3)}$$

Specific cell capacitance (C_{cell}, F g^{-1}) from CV curves

$$C_{cell} = \frac{\oint I\,dV}{4m \cdot S \cdot V_{tot}} \quad \cdots \quad \text{(Equation S4)}$$

Energy density (E_{cell}, Wh kg^{-1}) and power density (P_{cell}, kW kg^{-1})

$$E_{cell} = \frac{I}{2m \cdot 3.6}\int V dt \quad \cdots \quad \text{(Equation S5)}$$

$$P_{cell} = \frac{3.6\,E_{cell}}{\Delta t} \quad \cdots \quad \text{(Equation S6)}$$

where I is the applied current (A), $\int V\,dt$ is the integrated area under the non-linear discharge curve, corrected from the iR drop (V·s), ΔV is the voltage difference in the electrode (or cell) after the iR drop (V), $2m$ is the mass of two electrodes (g), S is the scan rate (V s^{-1}), V_{tot} is the operation voltage range (V), and Δt is the discharging time (s).

Criterion used to determine the electrochemical stability window

We determined the electrochemical stability window (or background limits) of the supporting electrolyte by the second-order derivative of the current with respect to the voltage ($d^2I/dV^2 < 3$) in the extended CV scan. The CV was measured at 20 mV s^{-1} in a three-electrode configuration with SWNT (0.4 mg), activated carbon (~ 10 mg) and Ag/Ag^+ as working, counter and reference electrodes, respectively. More than 20-fold higher mass activated carbon was used as the counter electrode for its smooth voltage shift. The CV was performed by increasing/decreasing the voltage range by 0.1 V until the rectangular CV shape starts to deviate noticeably. As the potential range expands into a positive/negative direction, the current value at the maximum/minimum potential ascend/descends steadily due to the resistance of the non-ideal EDLC (V=IR).[2] When the applied potential nears the voltage limitation (e.g. the electrolyte degradation), the corresponding current value exhibits a sudden increase/decrease. Therefore, the slope of the CV curve at the end point and the rate of this slope are key factors in defining the stable operation voltage window. In other words, the first- and second-derivative current change to voltage increase/decrease at the voltage end determines the electrochemical stability window of the supporting electrolyte. The first- and second-derivative current with respect to voltage are denoted as follows:

$$\frac{dI}{dV} = \frac{|I_2 - I_1|}{|V_2 - V_1|} \quad \cdots \quad \text{(Equation S7)}, \qquad \frac{d^2I}{dV^2} = \frac{d}{dV}\left(\frac{dI}{dV}\right) \quad \cdots \quad \text{(Equation S8)}$$

where I_2 and I_1 are the corresponding current values at the voltage end (V_2) and 0.1 V lower voltage than V_2 (V_1) of the CV curve, respectively.

To investigate the operation voltage window of supporting electrolyte (EMImTFSI/ADN), the current values (I_1 and I_2) at the voltage end and right before the end, the current change (dI), the first- (dI/dV), and the second-order derivative of current to voltage values (d^2I/dV^2) were tabulated in Table S1. In the positive voltage region, the current values show a steady upward trend, with the voltage extending to 1.4 V, but a severe deformation occurs at 1.5 V. This behavior indicates that the faradaic reaction occurs from 1.5 V, and the positive voltage would be restricted to 1.4 V, which is well matched with the potential of $TFSI^-$ oxidation from the literature. In the negative voltage region, the slope of the CV curves (dI/dV) remains almost constant down to -1.9 V (from 0.72 to 0.96). However, the voltage is scanned to further negative potential, the change rate of the slope exhibits a sudden incline at -2.0 V (d^2I/dV^2 = 3.69), resulting from the faradaic process. Therefore, the negative voltage was limited to -1.9 V, which is in good agreement with the ADN decomposition. From these evaluations, the electrochemical stability window can be determined by the second-derivative of current with respect to voltage (d^2I/dV^2) in CV curves, where its value is less than 3.

Table S1. Voltage ends, current values at the voltage end and right before end, current change, the first- and the second-order derivative values of current variation to voltage extension in CV curves of EMImTFSI/ADN (v = 20 mV s^{-1}).

Voltage (V *vs.* Ag/Ag^+)	**-2.1**	**-2.0**	**-1.9**	**-1.8**	**-1.7**	**-1.6**	**1.0**	**1.1**	**1.2**	**1.3**	**1.4**	**1.5**
I_2 (mA)	-1.42	-1.22	-1.11	-1.04	-0.98	-0.92	0.69	0.78	0.88	0.98	1.08	2.22
I_1 (mA)	-1.20	-1.09	-1.01	-0.96	-0.91	-0.85	0.63	0.70	0.79	0.87	0.94	1.12
dI (mA)	0.21	0.13	0.10	0.08	0.07	0.07	0.06	0.08	0.09	0.11	0.13	1.10
dI/dV	2.17	1.33	0.96	0.80	0.74	0.72	0.57	0.78	0.95	1.07	1.33	11.0
d^2I/dV^2	8.14	3.69	1.66	0.52	0.24		2.03	1.73	1.25	2.60	96.7	

Optimization of DmCc/DmCc$^+$ concentration.

An appropriate concentration of DmCc/DmCc$^+$ is required for stable operation of the DmCc/DmCc$^+$ supercapacitor. As described in the manuscript, the cell showed optimal performance with 0.04 M DmCc and 0.08 M DmCc$^+$. When the DmCc/DmCc$^+$ concentration is excessively low (e.g., 0.02 M DmCc & 0.04 M DmCc$^+$), the supercapacitor does not operate properly forming a partial voltage plateau, which disappears after several charge/discharge cycles (Figure S3). On the other hand, when the DmCc/DmCc$^+$ concentration is excessively high, DmCc/DmCc$^+$ precipitates out of the electrolyte solution.

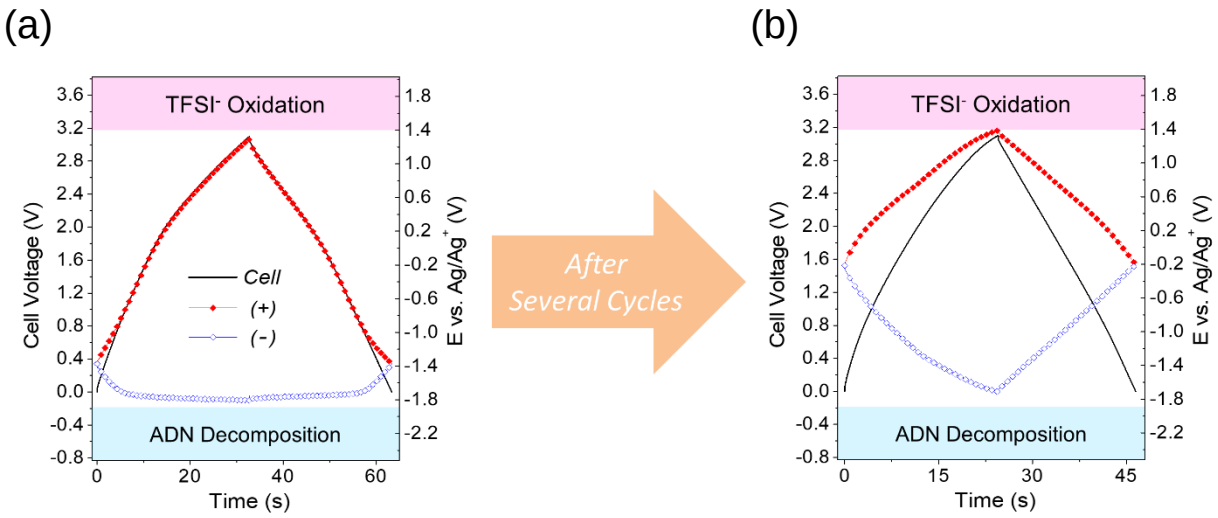

Figure S3. GCD graphs of a supercapacitor at the DmCc/DmCc$^+$ concentration of 0.02 M/0.04 M, (a) before and (b) after several cycles.

Estimation of the active mass of the redox species

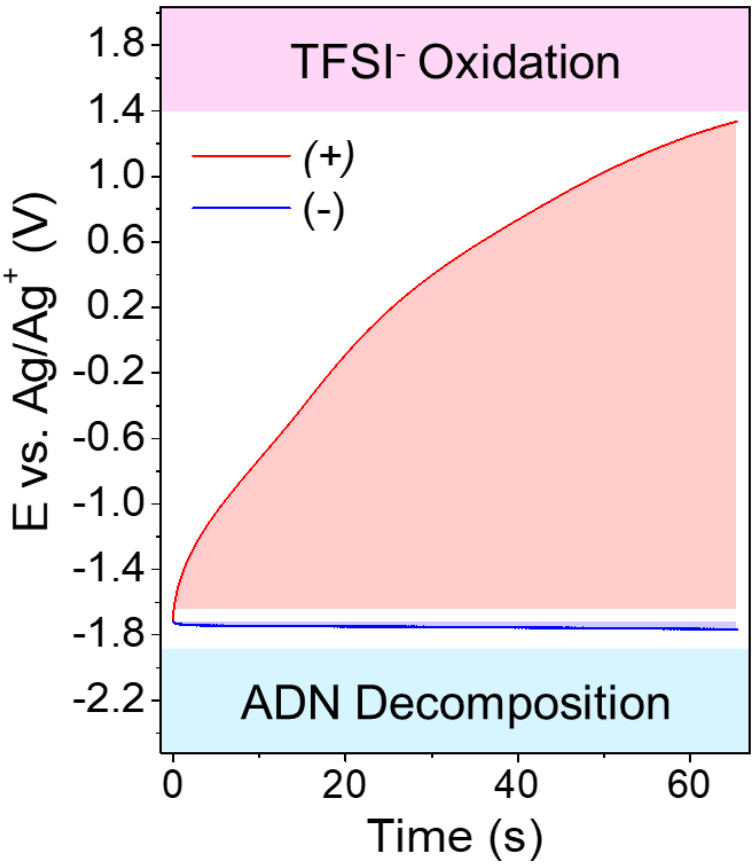

Figure S4. Enlarged GCD graphs with the voltage profiles of positive and negative electrodes in DmCc/DmCc$^+$/EMImTFSI/ADN during charging process (I = 2.5 A g^{-1}).

We estimated the active mass of the redox species from the amount of charge (Q) involved during charging process. Figure S4 shows the enlarged GCD graphs of positive and negative electrodes at the current density of 2.5 A g^{-1} for charging. As the amount of charge (Q) is proportional to the capacitance (C) and voltage variation (V), it is required to determine the capacitance (C_+ or C_-) and voltage variation corrected from the iR drop at each electrode (V_+ or V_-). For the realistic evaluation of non-linear GCD curves, the capacitance was calculated by the integration of GCD curves, following the equation:

$$C_+ \text{ or } C_- = \frac{I}{dV/dt} = \frac{I\int V\,dt}{\int V\,dV} = \frac{I\int V\,dt}{V^2/2|_0^{\Delta V}} = \frac{2I\int V\,dt}{V^2|_0^{\Delta V}} \quad \cdots \quad \text{(Equation S9)}$$

where I is the applied current (A), $\int V\,dt$ is the integrated area under the non-linear charge curve, corrected from the iR drop (V·s), ΔV is the voltage difference in the electrode after the iR drop (V). Therefore, the calculated capacitance of each electrode (C_+ and C_-) is 0.0575 and 4.18 F, respectively and the voltage variation of each electrode corrected from IR drop (V_+ and V_-) is 2.98 and 0.0417 V, respectively. The each amount of accumulated charge (Q_+ and Q_-) would be determined to be 0.172 and 0.175 C, which are almost the same.

Since the redox reaction ($DmCc^+ + e^- \rightarrow DmCc$) solely occurs at the negative electrode, the active mass of redox species could be calculated from the amount of accumulated charge at negative electrode (Q_-). As the capacitance from the redox reaction ($DmCc^+ + e^- \rightarrow DmCc$) would be much higher than that from EDLC ($EMIm^+$ & $DmCc^+$) at negative electrode, we assume that the accumulated charge from EDLC ($EMIm^+$ & $DmCc^+$) at negative electrode is negligible. Since the elementary charge and Avogadro constant are 1.60×10^{-19} C and 6.02×10^{23} mol^{-1}, respectively, the amount of transferred electrons is 1.81×10^{-6} mol. Since the reduction is one electron process, $DmCc^+$ is reduced to DmCc involving one electron transfer, the moles of $DmCc^+$ participated in redox reaction is the same as that of transferred electrons (= 1.81×10^{-6} mol). Therefore, from the molecular weight of $DmCc^+$ is ~329 g mol^{-1}, the mass of the active redox species ($DmCc^+$) is estimated to be approximately 0.6 mg.

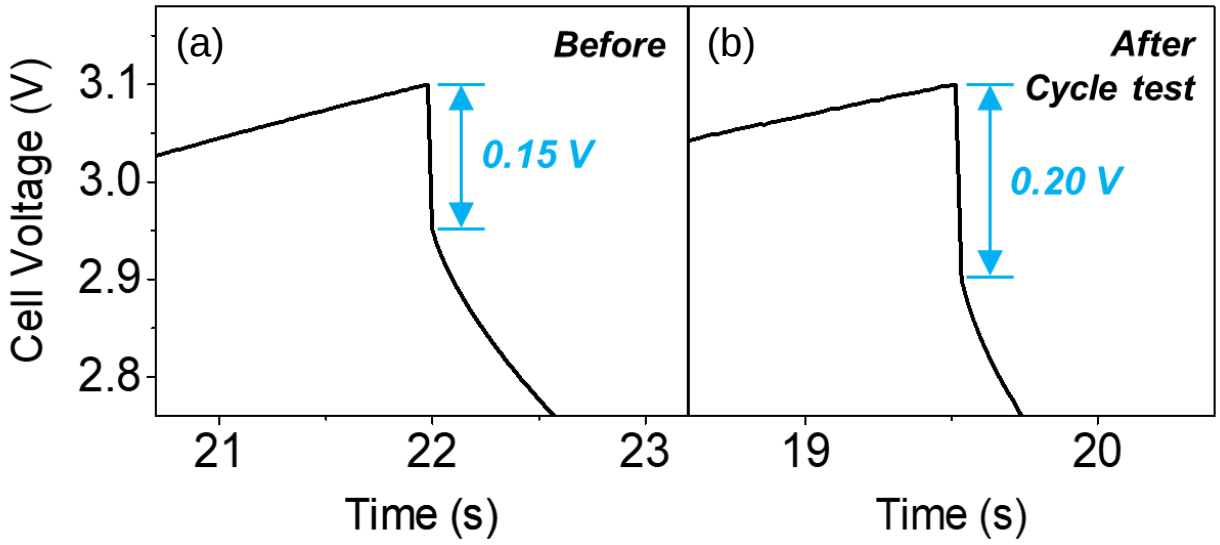

Figure S5. IR drops in GCD graphs (a) before and (b) after the cycle test of the supercapacitor with DmCc/DmCc^{+} (I = 5 A g^{-1}).

REFERENCES

1. Balducci, A.; Dugas, R.; Taberna, P.-L.; Simon, P.; Plee, D.; Mastragostino, M.; Passerini, S., High Temperature Carbon–Carbon Supercapacitor Using Ionic Liquid as Electrolyte. *J. Power Sources* **2007,** *165*, 922-927, DOI: 10.1016/j.jpowsour.2006.12.048.
2. Tanahashi, I., Comparison of the Characteristics of Electric Double-Layer Capacitors with an Activated Carbon Powder and an Activated Carbon Fiber. *J. Appl. Electrochem.* **2005,** *35*, 1067-1072, DOI: 10.1007/s10800-005-9002-1.